Int. J. Heat Mass Transfer. Vol. 10, pp. 567–580. Pergamon Press Ltd. 1967. Printed in Great Britain

LAMINAR FILM CONDENSATION ON THE UNDERSIDE OF HORIZONTAL AND INCLINED SURFACES

JOSEPH GERSTMANN* and PETER GRIFFITH†

(*Received* 1 *June* 1966 *and in revised form* 28 *September* 1966)

Abstract—Heat-transfer rates in laminar film condensation on the underside of horizontal and inclined surfaces are predicted by assuming the condensate flow to be the quasi-steady result of a bounded instability. This assumption makes it possible to determine the final shape of the liquid–vapor interface, and thus predict the average heat-transfer coefficient. Measurements of the heat-transfer coefficient obtained by condensing Freon-113 were found to agree quite well with the values predicted by this method.

Several distinct regimes of flow in the condensate film were observed. On the underside of horizontal surfaces, the interface is best described as a fully established Taylor instability. At slight angles of inclination there are three regimes of flow. Near the leading edge, the interface is smooth and waveless. Next there is a region of developing waves which are best described as elongated drops or longitudinal ridges. As the ridges grow in amplitude, drops form at the crests and subsequently fall from the surface. beyond the point at which drops first fall, a third regime exists which can be considered to be a fully developed state, independent of distance from the leading edge of the surface. At moderate angles of inclination and up to the vertical, "roll waves" appear a short distance from the leading edge.

NOMENCLATURE

(Dimensions in H, M, L, T, θ; Heat, Mass, Length, Time, and Temperature.)

c_p, specific heat at constant pressure [H/Mθ];
g, acceleration of gravity [L/T^2];
h_{fg}, heat of vaporization [H/M];
k, liquid thermal conductivity [H/LTθ];
L, length of condenser [L];
Nu, Nusselt number defined in equation (15);
p, pressure [M/LT^2];
p_{sat}, saturation pressure [M/LT^2];
Q/A, heat flux per unit area [H/L^{2}T];
r, radial coordinate, measured from axis of symmetry of drop [L];
Ra, modified Rayleigh number defined in equation (17);
ΔT, saturation temperature minus wall temperature [θ];
v_x, x-direction velocity [L/T];
v_z, z-direction velocity [L/T];
x, length coordinate parallel to surface [L];
z, length coordinate perpendicular to surface [L].

Greek symbols

δ, liquid film thickness [L];
δ_{max}, maximum film thickness [L];
δ_{min}, minimum film thickness [L];
θ, angle of inclination from a horizontal plane;
λ, wavelength [L];
Λ, dimensionless quantity defined in equation (11);
μ, liquid viscosity [M/LT];
ρ, liquid density [M/L^3];
ρ_v, vapor density [M/L^3];
σ, interfacial tension between liquid and vapor [M/T^2].

Superscripts

$'$, indicates differentiation with respect to $\hat{x}$ or $\hat{r}$;
$\bar{\ }$, indicates averaged quantity;

* Assistant Professor of Mechanical Engineering, Massachusetts Institute of Technology, Cambridge, Massachusetts.
† Associate Professor of Mechanical Engineering.

, indicates variable has been made dimensionless by division by $[\sigma/g(\rho - \rho_v)\cos\theta]^{\frac{1}{2}}$ or by δ_{min}.

INTRODUCTION

HEAT-TRANSFER rates in laminar film condensation on vertical, or near-vertical surfaces are adequately predicted by Nusselt's [1] analysis, or modifications of it taking into account the effects of interfacial shear, fluid acceleration, and non-linear temperature distribution. However, as surfaces are inclined more and more from the vertical, interfacial effects become important and one must now account for surface instabilities. In particular, a case in which interfacial instability plays the dominant role is that of film condensation on the underside of horizontal and slightly inclined surfaces. In a horizontal orientation, the film is unstable and forms pendent drops which increase in amplitude, eventually falling from the surface. This type of instability has been known as the Taylor instability [2]. If the surface is inclined, the condensate film flows along the surface in longitudinal "ridges". The ridges are themselves unstable, and drops form at the crests of ridges and eventually fall from the surface. Photographs of the interface at various inclinations are shown below.

The earliest attempt at predicting heat-transfer rates for horizontal surfaces was made by Popov [3] in 1951. His experimental data exhibited considerable scatter, possibly because of non-condensable gases. Both his theory and his experimental data give considerably lower heat-transfer coefficients than those of Gerstmann [4]. In 1960 Berenson [5] considered a similar problem, that of film boiling on the upper side of a horizontal surface. He assumed the boiling surface to be covered with hemispherical bubbles separated by areas of uniform film. The bubble spacing was determined by the Taylor wavelength, while the bubble sizes were determined from various experimental observations. He proposed that the mechanism of vapor removal was by radial laminar flow into the bubbles and showed that the momentum fluxes in the vapor could be neglected in comparison to viscous stresses. Except for the boundary condition on velocity at the liquid–vapor interface, Berenson's analysis would appear to be equally valid for film condensation on the underside of a horizontal surface. Although his results agree well with boiling data, the agreement is poor for condensation, even after corrections have been made for the differences at the interface.

Aside from the considerable effort in investigating the effects of waves on film condensation on vertical surfaces, there has been no work on condensation on the underside of inclined surfaces. For small inclinations from the horizontal, the wave state is characterized by longitudinal "ridges", with the bulk of the heat transfer occurring in the troughs of the ridges, while the downstream condensate flow is carried mainly in the ridges themselves. As the angle of inclination is increased, the wave state changes to one which is characterized by the flow of condensate in jagged sheets, as for example, in Fig. 9. These waves have been termed "roll-waves", by Hanratty and Hershman [6], who present an extensive survey of the literature in this area. Although the effects of roll-waves are by no means fully understood, the prime concern of this paper shall be the effects of pendent drops and ridges.

In the past, film boiling and similar phenomena have been analyzed by examining the stability of the unperturbed (waveless) state and then using the results of the stability analysis, notably the wavelength, to formulate a model representing the ultimate result of the instability. For example, Berenson [5] used the wavelength of the Taylor instability as the characteristic dimension of the vapor bubbles formed at the liquid–vapor interface during film boiling. The implication of this method is that the results of a perturbation analysis are still valid even when the perturbations are no longer small.

This analysis approaches the problem from a different point of view. Instead of examining the

unstable behavior of an initially unperturbed system, the ultimate state of the unstable system may be considered to be a steady state, the result of a bounded instability. The nature of this pseudo-steady state may then be determined by an ordinary equilibrium-type analysis. For example, instead of considering film condensation on the underside of a horizontal surface to be a case of a Taylor instability, it may be considered as non-linear interfacial instability whose rate of growth has been limited by viscosity. Limited, in fact, to such an extent that the flow in the condensate film is quasi-steady. If one has the necessary information to furnish sufficient boundary conditions, then one can solve for the shape of the liquid–vapor interface and thus the heat-transfer coefficient. The only assumptions as to the shape of the interface need be of a qualitative nature, such as whether the interfacial waves have line or cylindrical symmetry. This information may be obtained from a simple experimental observation.

EXPERIMENTS

Apparatus

The experimental program had a twofold purpose. First, as the heat-transfer analysis would require the formulation of a model of the condensate film, the experiments were to provide qualitative information about the nature of the liquid–vapor interface. Second, quantitative heat-transfer data would indicate the accuracy of the analysis. The apparatus, shown in Fig. 1, consisted of a water-cooled copper condensing surface, a Pyrex condensing chamber with resistance heaters, reflux condensers for condensation and degassing of excess vapor, and a coolant flow loop.

The condensing surface, measuring 18 × 6 in, was the uninsulated face of a 2-in thick copper bar. The other faces were insulated with 2 in of poly-foam insulation, sealed with epoxy resin. Cooling water flowed through twenty-four half-inch diameter coolant passages in the copper bar, connected in series. The temperature rise of the coolant was measured between the inlet and outlet with a ten-junction, copper–constantan thermopile. The surface temperature was measured with four copper–constantan thermocouples located within a nominal distance of $\frac{1}{16}$ in of the test surface, and equally spaced along the test section.

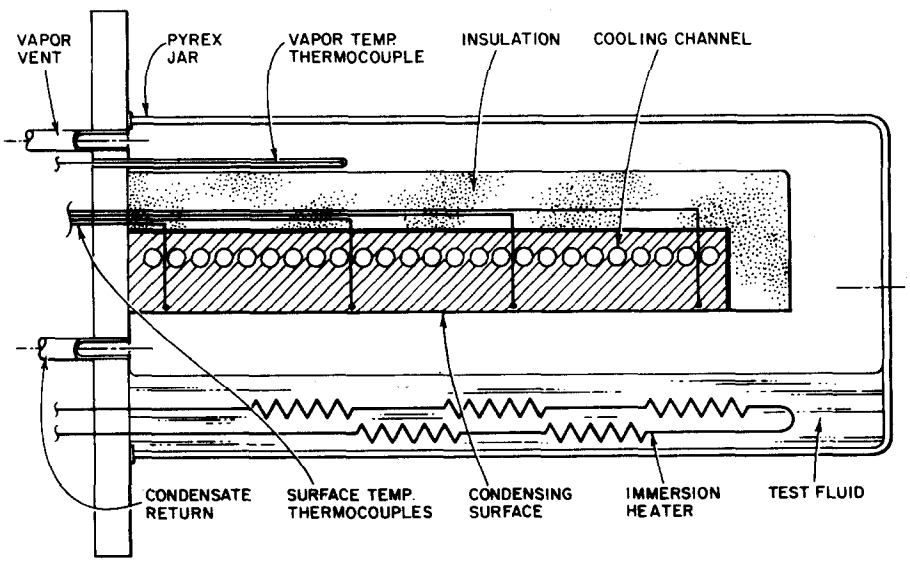

FIG. 1. Experimental apparatus.

The condensing chamber was formed by a 15-gal Pyrex tank and a Bakelite cover plate to which the copper test section was bolted. The entire apparatus could be rotated about a horizontal axis. Resistance heaters at the bottom of the tank boiled the test fluid, Freon-113. A thermocouple located just above the test section measured the temperature of the saturated vapor, which was maintained just above atmospheric pressure by venting through the reflux condensers. Of the vapor generated by the resistance heaters, about half was condensed on the test surface. The remainder passed through the primary reflux condenser where almost all of it was condensed, the condensate returning to the condensing chamber. The residual vapor plus any non-condensable gases went to a secondary condenser where the residual condensate was removed from the system and any non-condensable gases were vented to the atmosphere. In this manner, the vapor was continually stripped of non-condensable gases and the two-condenser system minimized the amount of air leaking into the condensing chamber by being dissolved in the returning condensate.

The cooling water was circulated through the system from a 40-gal reservoir. The tests were started with the water at 32°F, and it was allowed increase in temperature during the tests at the rate of one degree every 3–10 min. The water flow rate was measured by a Brooks Rotameter, calibrated to ± 1 per cent.

Heat-transfer rates were determined from measurements of the flow rate and temperature rise of the coolant. The temperature difference between the test surface and the saturated vapor was obtained from the thermocouple measurements. The details of the experimental procedure and the original measurements may be found in reference [7].

Horizontal test results

The experiments on condensation of Freon-113 on the underside of the horizontal surface covered heat-transfer rates from 1640 to 8030 Btu/ft^2 h and temperature differences ranging from 7·8 to 56·5 degF. These data are shown in Fig. 2.

The condensing interface, as shown in Fig. 3, is best described as consisting of an apparently random array of "cosine-shaped" drops. Even though the condensing surface is horizontal, the drops are not stationary, but meander about due to the disturbances of neighboring drops.

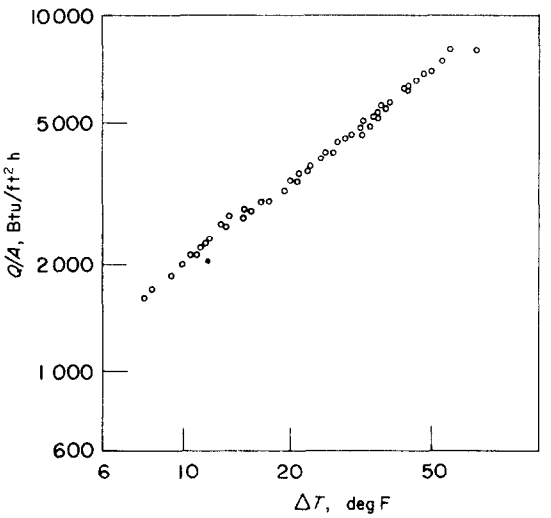

FIG. 2. Horizontal heat-transfer data.

Motion pictures of the interface show that new drops grow from the same sites vacated by fallen drops. Alternate growth and departure at neighboring sites, found in film boiling on a wire by Lienhard and Wong [8], was not observed. The number of drops per unit area increases slightly with heat flux, due mainly to the fact that there is less coalescence of drops at the higher heat fluxes. At heat fluxes above, 4000 Btu/ft^2 h, the number of drops remained roughly constant at 6·5 drops per square inch for Freon-113 at 1 atm.

The nature of the interface during steady condensation differs significantly from that during a transient formation of condensate on an initially dry surface. Figure 3 may be compared with Fig. 4 which is a 15-s sequence taken when

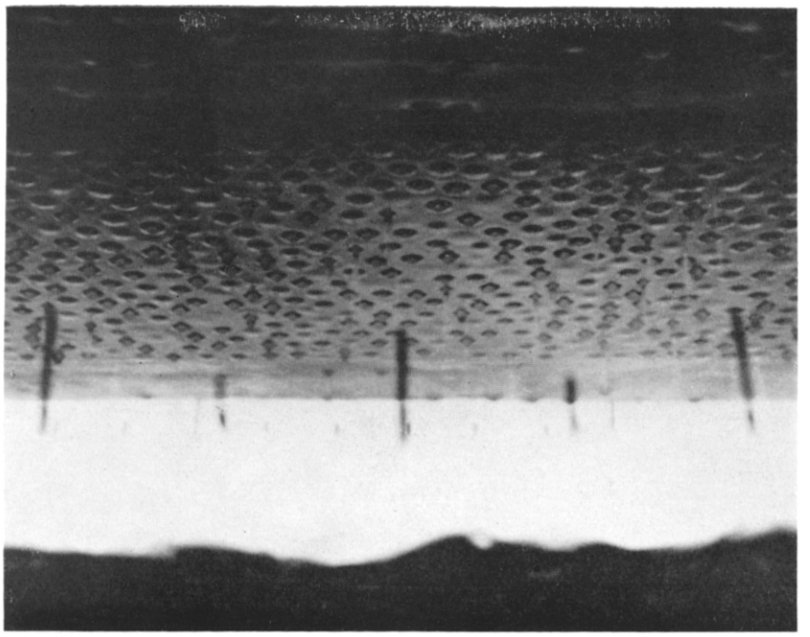

FIG. 3. Horizontal, drop-type condensation.

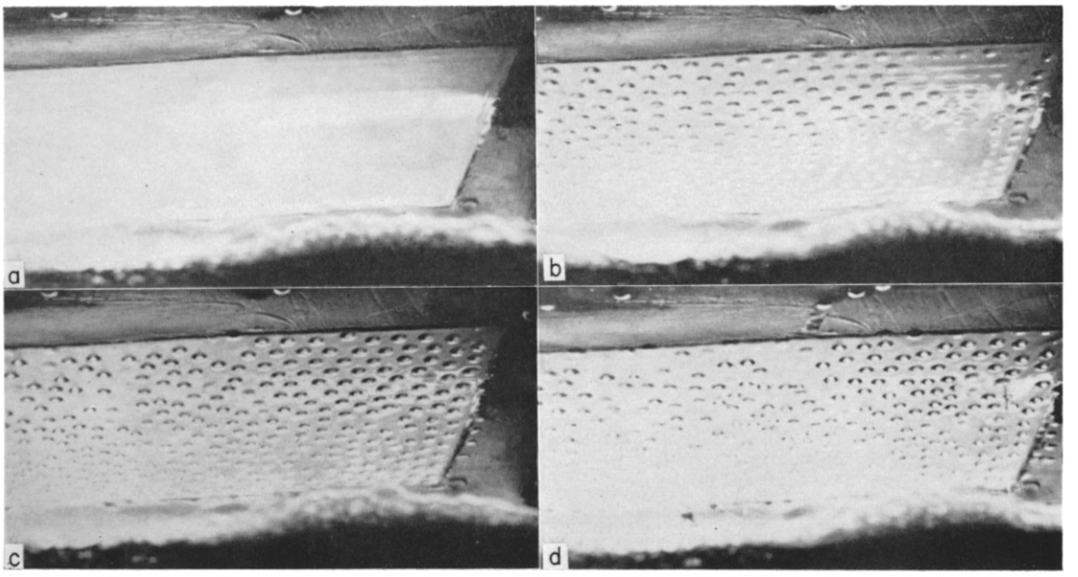

FIG. 4. Transient condensation: (a) smooth film with ridges forming at boundaries; (b) ridges developing into drops; (c) close-packed drop pattern; (d) break-up of close-packed pattern.

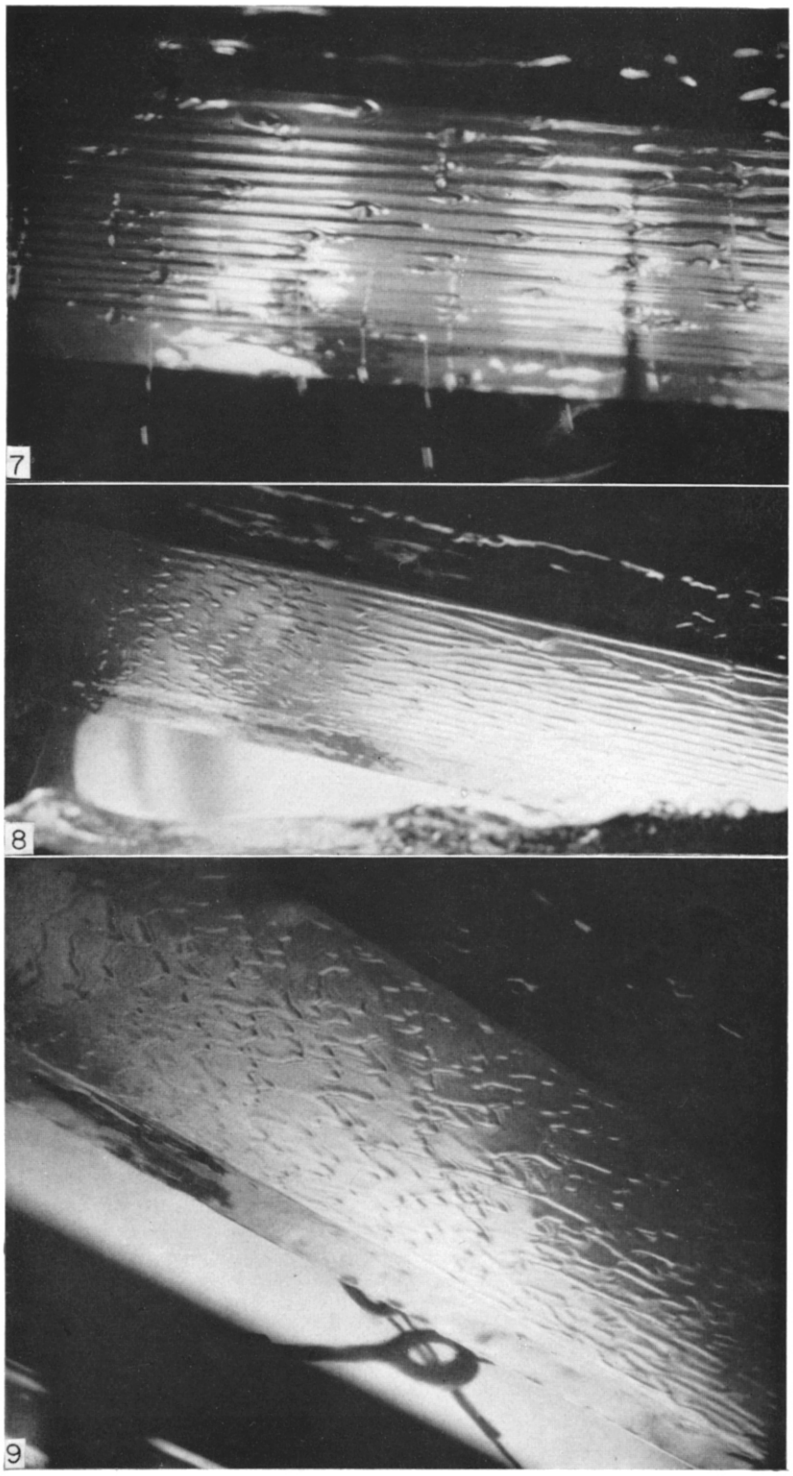

FIG. 7. Inclined, fully-developed ridge-type condensation.
FIG. 8. Inclined, developing ridge-type condensation.
FIG. 9. Inclined, roll-wave condensation.

the test surface was suddenly cooled to below saturation temperature. Initially, a smooth, waveless film appears on the surface. Next, disturbances originating at the boundaries of the surface move inward to the center of the test surface, forming a regular standing wave pattern which develops into a close-packed pattern of drops. Near the corners of the surface, the uniformity is disrupted, indicated the strong effects of the boundaries. However, after several drops have fallen from the surface, a regular drop packing is no longer evident and the boundaries appear to have lost their influence.

Effects of non-condensable gases

In all investigations of this type, the question arises as to whether the tests were free of the effects of non-condensable gases. Elaborate precautions are always necessary to rid a system of these gases. Care was always taken to see that the Freon–air interface was kept in the secondary condenser, so that the condensate in the primary reflux condenser would contain only pure Freon plus traces of non-condensables in the process of being removed from the system. The effectiveness of this system was checked by allowing the Freon–air interface to retreat from the secondary condenser to the primary, thus allowing the possibility of dissolved air entering the test chamber via the returning condensate. There was an immediate effect on the condensation on the test surface. If the surface was horizontal, regions which had previously been covered with drops became drop-free. Instead, the film would have a random, ripply motion at the interface with the occasional formation of a solitary drop. There was also a considerable decrease in heat-transfer rate.

The reason for the above behavior has been explained by Trefethen [9], as follows: Because of the bulk motion of vapor towards the interface, a concentration gradient of the non-condensable gas is set up with a maximum concentration at the interface. The concentration at the interface is highest where the local heat-transfer rate is highest, i.e. where the condensate film is thinnest. If we perturb the film at a point so that it starts to increase in thickness, the heat-transfer rate, hence the concentration, will diminish at the point. Since the concentration is in direct proportion to the partial pressure, and the total pressure remains constant, the partial pressure of the condensing vapor will increase, as will the saturation temperature. The rise in temperature of the interface will result in a lowering of the surface tension. The resulting surface tension gradient gives rise to a flow of condensate away from the point under consideration, thus diminishing the rate of growth of the perturbation. In this respect, it is seen that non-condensables have a stabilizing effect on the interface.

Because of the drastic difference in the appearance of the interface in the presence of non-condensable gases, we feel quite certain that the results presented in this work are free of the effects of non-condensable gases.

Inclined test results

The heat-transfer data for condensation of Freon-113 on the underside of the test surface inclined at $2\frac{3}{4}°$ and 5° from the horizontal are shown in Fig. 5. The data for inclinations between $7\frac{1}{2}°$ and 90° are given in Fig. 6. Qualitatively, the interface is similar to that for a

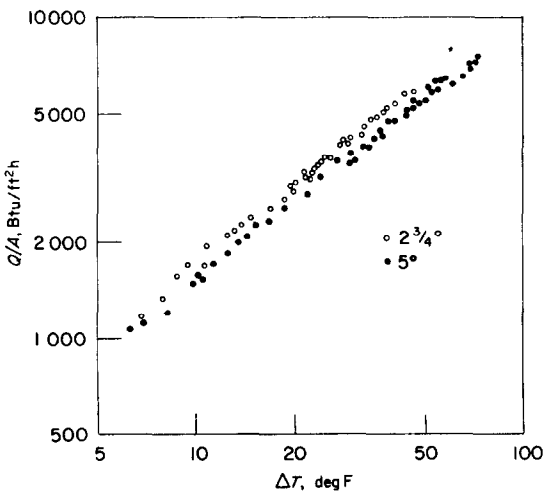

FIG. 5. Inclined heat-transfer data at $2\frac{3}{4}°$ and 5°.

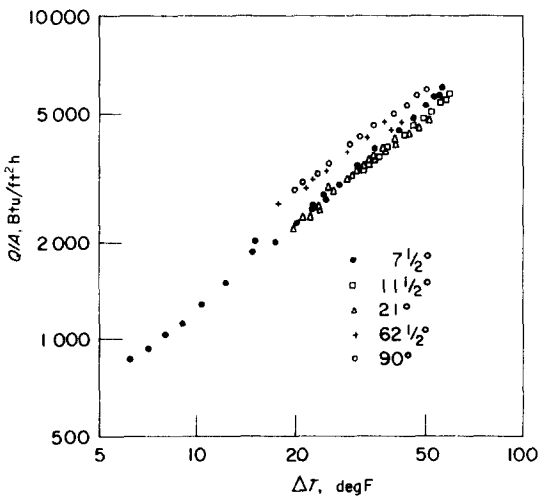

FIG. 6. Inclined heat-transfer data from $7\frac{1}{2}°$ to 90°.

horizontal surface. Beyond a short waveless region near the leading edge of the surface, droplike disturbances form. The disturbances become elongated as they move downstream and grow in amplitude until drops fall from the interface. At about the point that drops fall from the surface, the interface more closely resembles ridges than elongated drops. Beyond the point at which drops first fall, the nature of the interface appears to be independent of distance from the leading edge. Figure 7 is a photograph of this "fully developed" region taken at an inclination of 5°. For all angles at which ridges were observed, there were seventeen ridges across the 6-in width of the surface.

As the angle of inclination is increased, the nature of the interface changes. This is illustrated by Figs. 8 and 9 which depict the interface at inclinations of 13° and $19\frac{1}{2}°$. Figure 8 is similar to Fig. 7 insofar as the interface is composed of ridges. However, the ridges are now not as straight as before, and neighboring ridges occasionally collide. Furthermore, although the heat flux is about the same, no drops fall from the interface. Instead, all the condensate runs off the end of the test surface. In Fig. 9, the interface no longer is ridge-like, but is composed of jagged sheets which resemble roll waves. At angles greater than 20°, the qualitative nature of the interface is unchanged, even up to 90°.

Regimes of flow

In the experiments described above, we may classify the horizontal and slightly inclined flows as being four basically different types. First there is the situation which exists when the condensing surface is horizontal; here there is no preferred direction to the flow nor any characteristic dimension impressed upon the flow by the system. That is, the dimensions of the condensing plate do not affect the hydrodynamics, thus the state of the film does not depend upon the distance from a particular boundary. Here the flow is dominated by the presence of pendent drops, and the flow is essentially radial into the drops.

Second there are the states of flow which are determined by the angle of inclination and the distance from the leading edge of the plate. These may be classified into three groups. The first is the glassy, smooth flow which exists near the leading edge of the plate, where the disturbances are of extremely small amplitude. The second is the developing wave state where the disturbances are of appreciable amplitude but there is no rupture of the interface (i.e. no drops have fallen from the surface). Third there is the state which exists beyond the point at which the interface has first ruptured, where it is reasonable to expect that the flow is now independent of the distance from the leading edge, although there may be a periodic dependence on the longitudinal direction. Although the lines of demarkation between all of the classes but the last are quite hazy, a qualitative separation is possible.

The most difficult distinction is between the horizontal, drop dominated flow, and the inclined, ridge-type flow. For even when the surface is slightly tilted, and the drops run in one direction and become slightly elongated, one does not observe a significant difference in the heat-transfer rate, nor can one say that the interface is ridge-like. However, we can say with

some degree of definiteness that at 1° the surface is still droplike, while at 4°, the disturbances must be called ridges rather than drops.

The remaining three regimes are mapped in Fig. 10 for angles of $2\frac{3}{4}°$, 5°, and $7\frac{1}{2}°$. It is seen that in all cases the transition points move downstream with increasing angle and decreasing heat flux.

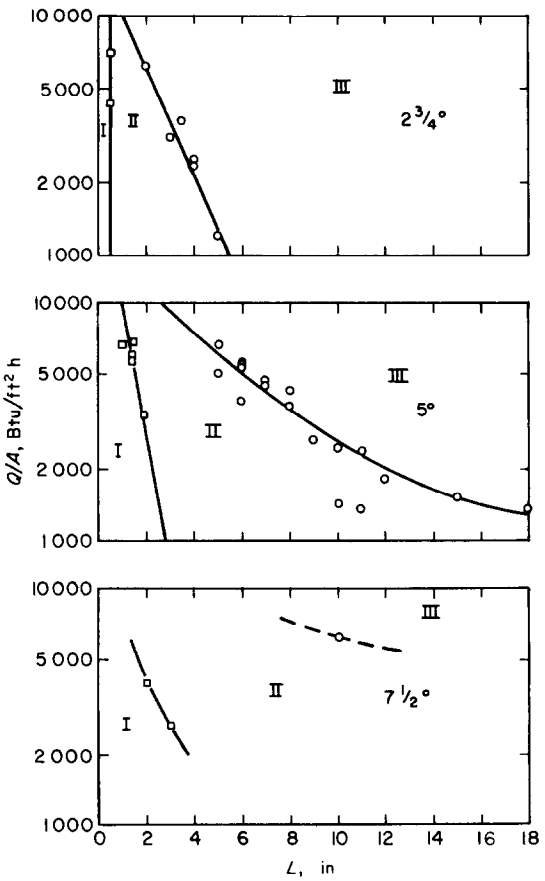

FIG. 10. Flow regimes in inclined condensation: I, waveless flow; II, developing flow; III, fully developed, ridge-type flow.

ANALYSIS

Formulation of the problem

The problem of predicting the average heat-transfer coefficient for the unstable condensate film is complicated by the fact that we must analyze the transient behavior of an unstable, three-dimensional, non-linear system. If it is assumed that the instability is bounded and that the flow in the condensate film is quasi-steady, then the problem is greatly simplified. For the horizontal case, this implies that, except for the short period of time during which a drop is breaking away from the surface, the amplitude of the interfacial waves may be characterized by a certain mean drop height. Conceptually, we may force the flow to be steady by imagining a line sink to be located at the center of each drop. If we further idealize the problem by assuming that the flow has cylindrical symmetry about the vertical axis of each drop, then we obtain the further simplification of two-dimensionality.

For the case of condensation on the underside of inclined surfaces some insight into the problem may be gained by dividing the film into two regions, a region of thin film and a region of thick film. In the thin film between the crests of the ridges the bulk of the heat transfer occurs and the flow is governed by a balance of surface forces to viscous forces. In the thick film, there is little condensation and viscous forces are much smaller than in the thin film region. Furthermore, if the bulk of the condensation occurs in the thin film region and yet the condensate is removed by the formation of drops at the crests of the ridges, then in the thin film, the condensate must flow transversely into the ridges. Downstream of the point at which drops first fall from the interface, we may assume that, in the thin film, there is no downstream flow, and that the flow is fully-developed in the downstream direction. If, as above, we make the further idealization that the flow is steady, then one comes to the conclusion that in the region of thick film, the transverse profile of the interface must be governed by the balance of surface to gravitational forces, and the downstream flow does not affect this profile.

The condition of steady flow may be satisfied if it is imagined that a plane sink is located at the center-line of each ridge. This makes it

possible to replace the actual method of condensate removal by falling drops, by the artifice of steady flow into the plane sink. The net result of all of the above idealizations is that it is now necessary to consider the condensate flow in two dimensions only.

Although the "steady-state" assumption greatly simplifies the analysis, it also destroys some information, since the amplitude of the surface waves, which is in reality a function of time, is now unknown. This situation must be remedied by specifying the average height of the drops or ridges in the form of a boundary condition. From experimental observation, it is found that amplitudes of the drops and ridges are of the order of the wavelength of the instabilities. There is some theoretical basis for this observation in the work of Bashforth and Adams [10]. Their calculations of the shapes of pendent drops show that the volume of a pendent drop having zero contact angle reaches a maximum when the height of the drop, δ_{max}, is equal to 2·24 $[\sigma/g(\rho - \rho_v)]^{\frac{1}{2}}$. If we interpret this to mean that a further increase in amplitude (or volume) renders the drop unstable, then the average drop (or ridge) found on the condensing surface will have a height somewhat less than 2·24 $[\sigma/g(\rho - \rho_v)]^{\frac{1}{2}}$.

Since the shortest unstable wavelength of the Taylor Instability is $2\pi\ [\sigma/g(\rho - \rho_v)]^{\frac{1}{2}}$, [8], the amplitude and the wavelength will be of the same order. For this analysis, we will assume that

$$\delta_{max} = [\sigma/g \cos\theta(\rho - \rho_v)]^{\frac{1}{2}} \qquad (1)$$

where g has been replaced by $g \cos\theta$, the component of gravity normal to the surface. At the conclusion of the analysis it will be seen that the prediction of the heat-transfer coefficient is sensitive only to the order of magnitude of the amplitude and not to its exact value.

Inclined surfaces

In addition to the assumptions of the previous section the following assumptions are made:

1. The flow is laminar.
2. The angle of inclination, θ, is small.
3. The pressure in the film is hydrostatic.
4. The vapor exerts negligible shear on the interface.
5. The wall temperature and the vapor temperature are uniform.
6. The group $k\,\Delta T/\mu h_{fg}$ is much less than unity.
7. The group $c_p\,\Delta T/h_{fg}$ is much less than unity.

The net effect of the above assumptions is to make the flow two-dimensional and to make the velocity profiles similar at all sections. As a result of assumption 6, which may be shown to be equivalent to the assumption of small Reynolds number, the momentum fluxes in the liquid film may be neglected, requiring a balance of the pressure gradient with the viscous stresses in the thin film [equation (2)]. Furthermore, assumption 2, along with the observation that the curvature along the ridges (y-direction) is small, requires that the y-direction flow be small compared to the x-direction flow (normal to the ridges). The assumption that the pressure is hydrostatic [equation (3)] enables one to determine the velocity in terms of the film thickness, which, when the condensate flow rate is expressed in terms of the heat-transfer rate, enables one to express the average heat-transfer rate in terms of the film-thickness, [equations (10) and (12)].

For the model of the interface shown in Fig. 11 and under the assumptions listed above, the governing equations are:

$$\frac{\partial p}{\partial x} = \mu \frac{\partial^2 v_x}{\partial z^2}, \qquad (2)$$

$$p = p_{sat} - (\rho - \rho_v)\, g \cos\theta\, (\delta - z) - \sigma \frac{\mathrm{d}^2\delta}{\mathrm{d}x^2}, \qquad (3)$$

$$\frac{\partial v_x}{\partial x} + \frac{\partial v_z}{\partial z} = 0, \qquad (4)$$

and

$$Q/A = k\,\Delta T/\delta. \qquad (5)$$

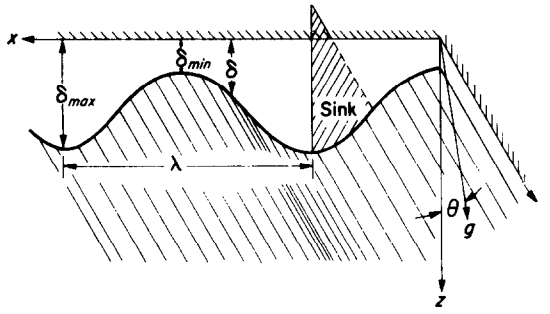

FIG. 11. Ridge model.

By differentiating equation (3) and substituting the result into equation (2) the relationship between velocity and film thickness is found to be

$$\mu \frac{\partial^2 v_x}{\partial z^2} = -(\rho - \rho_v) g \cos\theta \frac{\mathrm{d}\delta}{\mathrm{d}x} - \sigma \frac{\mathrm{d}^3\delta}{\mathrm{d}x^3}. \quad (6)$$

Equation (6) may now be integrated over the film thickness using the boundary conditions of zero velocity at the wall and zero shear at the interface to obtain

$$v_x = \frac{\delta^2}{2\mu}\left[(\rho - \rho_v) g \cos\theta \frac{\mathrm{d}\delta}{\mathrm{d}x} + \sigma \frac{\mathrm{d}^3\delta}{\mathrm{d}x^3}\right] \times \left[\frac{2z}{\delta} - \frac{z^2}{\delta^2}\right]. \quad (7)$$

By integrating equation (4) over the film thickness, δ, and making use of the relationship between the condensation rate and the velocities at the interface, namely

$$\left[v_x \mathrm{d}\delta - v_z \mathrm{d}x = \frac{Q/A}{\rho h_{fg}} \mathrm{d}x\right]_{z=\delta} \quad (8)$$

we arrive at

$$\frac{\mathrm{d}}{\mathrm{d}x} \int_0^\delta v_x \mathrm{d}z = \frac{Q/A}{\rho h_{fg}}. \quad (9)$$

Equations (5) and (7) are used to evaluate the above integral to get

$$\frac{\mathrm{d}}{\mathrm{d}x}\left\{\left[(\rho - \rho_v) g \cos\theta \frac{\mathrm{d}\delta}{\mathrm{d}x} + \sigma \frac{\mathrm{d}^3\delta}{\mathrm{d}x^3}\right] \frac{\delta^3}{3\mu}\right\} = \frac{k\,\Delta T}{\delta \rho h_{fg}}. \quad (10)$$

Equation (10) can be made dimensionless by defining the following new variables:

$$\hat{\delta} = \delta/\delta_{\min}, \qquad \hat{x} = x/[\sigma/g(\rho - \rho_v)\cos\theta]^{\frac{1}{2}},$$
$$\Lambda = \frac{k\,\Delta T \sigma \mu}{\rho h_{fg}[g(\rho - \rho_v)\cos\theta]^2 \delta_{\min}^5}. \quad (11)$$

Using primes to signify differentiation with respect to $\hat{x}$, equation (10) may be restated as

$$\hat{\delta}^4[\hat{\delta}'''' + \hat{\delta}''] + 3\hat{\delta}^3[\hat{\delta}''' \hat{\delta}' + (\hat{\delta}')^2] = 3\Lambda. \quad (12)$$

By using $\delta_{\min}$ as the characteristic dimension of the film thickness, it is possible to completely specify the problem as an initial value problem. Two of the initial values are obtained from symmetry considerations; namely that the first and third derivatives must be zero at the point of minimum film thickness. A third is that the dimensionless film thickness must be unity, by definition, at the minimum point. The fourth comes from the observation that the curvature vanishes at the point of minimum thickness. (A good example of this may be seen in Fig. 3). Note that because the plane sink requires a finite velocity at the point of maximum film thickness, the conditions of symmetry do not hold at the crests of the ridges. Thus the initial values required for the solution of equation (12) are

$$\text{at } \hat{x} = 0: \quad \hat{\delta} = 1, \quad \hat{\delta}' = 0, \quad \hat{\delta}'' = 0, \quad \hat{\delta}''' = 0. \quad (13)$$

Equation (12) was solved numerically [7] on an IBM 7094 digital computer. The results of the computation, for values of Λ ranging from 200 to 6400 are summarized in Table 1. Here, $\hat{\lambda}/2$ is the value of $\hat{x}$ at which the film thickness

Table 1. Computed results for ridge model

Λ	$\hat{\lambda}/2$	$\delta_{\max}$	$\overline{Nu}$	Ra
200	3·417	73·66	12·62	$1·084 \times 10^7$
400	3·373	103·7	15·01	$2·99 \times 10^7$
800	3·336	146·2	17·95	$8·33 \times 10^7$
1600	3·305	206·4	21·45	$2·31 \times 10^8$
3200	3·279	291·0	25·45	$6·49 \times 10^8$
6400	3·255	410·0	30·25	$1·81 \times 10^9$

reaches a maximum. Combining the computed value for $\hat{\delta}_{max}$ with equation (1), the value of $\hat{\delta}_{min}$ may be obtained from the expression

$$\delta_{min} = \frac{[\sigma/g(\rho - \rho_v)\cos\theta]^{\frac{1}{2}}}{\hat{\delta}_{max}}. \tag{14}$$

Defining the Nusselt number to be

$$Nu \equiv \frac{h}{k}\left(\frac{\sigma}{g(\rho - \rho_v)\cos\theta}\right)^{\frac{1}{2}} \tag{15}$$

and by expressing h in terms of equation (5), the average Nusselt number may be expressed as

$$\overline{Nu} = \frac{2\hat{\delta}_{max}}{\hat{\lambda}} \int_0^{\hat{\lambda}/2} \frac{d\hat{x}}{\hat{\delta}}. \tag{16}$$

Since the quantity Λ, which appears in equation (12) as a parameter, is actually a variable as it contains the unknown δ_{min}, equation (14) must be used to eliminate δ_{min} from Λ. It is then possible to express the average Nusselt number as a function of the modified Rayleigh number.

$$Ra = \frac{g\cos\theta\,\rho(\rho - \rho_v)\,h_{fg}}{k\mu\,\Delta T} \cdot \left[\frac{\sigma}{g(\rho - \rho_v)\cos\theta}\right]^{\frac{3}{2}}. \tag{17}$$

The results of the numerical integration of equation (16) and the evaluation of the Rayleigh numbers for given values of Λ are presented in Table 1. It is interesting to note that the minimum film thickness, as expressed by the reciprocal of $\hat{\delta}_{max}$, is typically two orders of magnitude less than the ridge amplitude.

In separate analysis [7] which involved the linearization of equation (12), it has been shown that the Nusselt numbers in Table 1 may be expressed as

$$\overline{Nu} = 0{\cdot}90\,(Ra)^{\frac{1}{4}}/[1 + 1{\cdot}1\,(Ra)^{-\frac{1}{4}}] \tag{18}$$

if the value of the Rayleigh number is greater than 10^6.

If the assumption that the maximum ridge height is given by equation (1) is incorrect, then it can be shown by direct substitution that an error of 100 per cent in the value of δ_{max} results in an error of only 11 per cent in equation (18).

Horizontal surfaces

The analysis of condensation on the underside of horizontal surfaces is similar to that for inclined surfaces, the only basic difference being cylindrical symmetry as opposed to line symmetry. Omitting the derivation, the differential equation for the interface is [7]

$$\hat{\delta}^4[\hat{\delta}'''' + \hat{\delta}'' + 2\hat{\delta}'''/\hat{r} + \hat{\delta}'/\hat{r} - \hat{\delta}''/\hat{r}^2 + \hat{\delta}'/\hat{r}^3] + 3\hat{\delta}^3[\hat{\delta}'''\hat{\delta}' + (\hat{\delta}')^2 + \hat{\delta}''\hat{\delta}'/\hat{r} - (\hat{\delta}')^2/\hat{r}^2] = 3\Lambda \tag{19}$$

where the primes indicate differentiation with respect to $\hat{r}$. The initial conditions used to integrate this equation were:

$$\text{at } \hat{r} = \hat{\lambda}/2; \quad \hat{\delta} = 1; \quad \hat{\delta}' = 0; \quad \hat{\delta}'' = 0; \quad \hat{\delta}''' = 0. \tag{20}$$

As the radius appears explicitly in equation (19), the value of the wavelength is needed in order to apply the initial conditions. This problem was circumvented by guessing a value of the wavelength, integrating equation (19), and retaining only those wavelengths which give zero slope at or near $\hat{r} = 0$. The integration could not be carried out all the way to $\hat{r} = 0$ since the left hand side of equation (19) becomes infinite at this point. This is because the line sink at $\hat{r} = 0$ requires either infinite film thickness or infinite velocity at $\hat{r} = 0$. However, a very short distance away from the origin, at a radius of less than 8 per cent of the maximum drop radius, the velocities are extremely small, and the shape of the interface is controlled solely by the balance of surface and gravity forces. The Nusselt numbers were calculated according to the formula

$$\overline{Nu} = \frac{4\hat{\delta}_{max}}{\pi\hat{\lambda}^2} \int_0^{\hat{\lambda}/2} \frac{2\pi\hat{r}\,d\hat{r}}{\hat{\delta}}. \tag{21}$$

The results of this calculation may be expressed as

$$\overline{Nu} = 0{\cdot}81\,(Ra)^{0{\cdot}193}; \qquad 10^{10} > Ra > 10^{8};$$
$$\overline{Nu} = 0{\cdot}69\,(Ra)^{0{\cdot}20}; \qquad 10^{8} > Ra > 10^{6}. \tag{22}$$

DISCUSSION

In Fig. 12 the experimental results are compared with the theory for horizontal and slightly inclined surfaces. The horizontal data fall from 10 to 15 per cent below the theoretical curve. The data at $2\frac{3}{4}°$ fall somewhat above the values predicted by equation (18), while at 5°, the data fall below the theory. The fact that the data at $2\frac{3}{4}°$ lies in between the theories for horizontal and inclined condensation is to be expected, since at this angle the film is in the transition region between horizontal, drop-type flow and inclined, ridge-type flow. The 5° data, however, represent a fully established, ridge-type flow.

The main cause of the 10–15 per cent disagreement between the theory and experiment appears to stem from the steady-state assumption. This manifests itself in the underestimation of the wavelength. At a Rayleigh number of 10^7, Table 1 requires a wavelength, $\hat{\lambda}$, of 6·8 for the ridges, while the calculated value for a drop on a horizontal surface [7], is 8·6. The measured wavelengths are 8·7 and 10·9, about 25 per cent higher. Thus the observed wavelengths fall in between the wavelengths for neutral stability predicted by this analysis and the "most-unstable" wavelengths, which, for the case of two dimensional instabilities, are greater by a factor of $\sqrt{3}$ than the neutral wavelengths.

The data for inclinations between $7\frac{1}{2}°$ and 90° are plotted separately in Fig. 13. These data are compared with the modification [11] of Nusselt's [1] theory for condensation on a vertical surface:

$$\frac{\bar{h}L}{k} = 0{\cdot}943 \times \left[\frac{g\sin\theta\,\rho(\rho-\rho_v)\,L^3(h_{fg}+0{\cdot}68\,c_p\,\Delta T)}{k\mu\,\Delta T}\right]^{\frac{1}{4}}. \tag{23}$$

For vertical surfaces, the net effect of the roll waves is an increase in the Nusselt number by about 10 per cent above that predicted by equation (23). This increase remains roughly constant up to an inclination of about 20° from the horizontal. This result substantiates the earlier observation that the interfacial waves appear to be unchanged between angles of

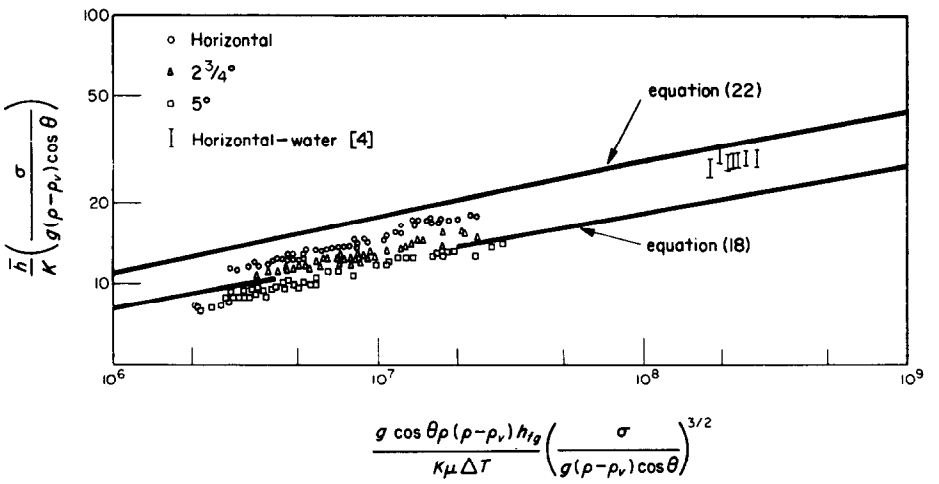

FIG. 12. Comparison of data at small inclinations with equations (18) and (22).

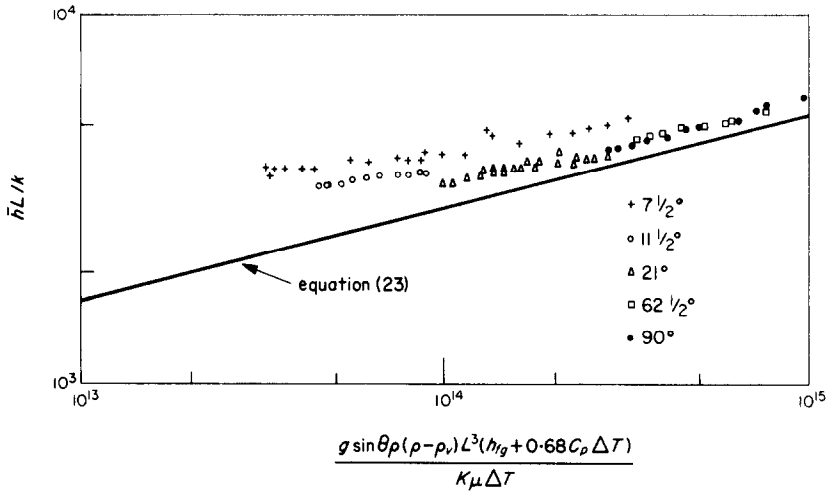

FIG. 13. Comparison of data at large inclinations with equation (23).

20° and 90°. On the other hand, the data at $7\frac{1}{2}°$ and $11\frac{1}{2}°$ deviate significantly from equation (23). At these inclinations, most of the surface is composed of developing ridges with no drops falling from the surface. It therefore lies in the transition region between flow with shallow roll waves as characterized by equation (23) and fully developed ridge-type flow as characterized by equation (18).

CONCLUSIONS

(1) In condensation on the undersides of horizontal and inclined surfaces, several distinct flow regimes exist. However, the common feature of these regimes is the flow of condensate from a thin-film region into a ridge or drop. For inclined surfaces, the transverse flow of condensate into fully developed ridges differs from the radial flow into pendent drops of horizontal surfaces only as line symmetry differs from cylindrical symmetry. Basically, the phenomenon may be described as a Taylor instability whose rate of growth has been limited by viscosity.

(2) Although the phenomenon is basically an instability, the condensation rate may be predicted by assuming the flow to be steady. This assumption gives good results for horizontal condensation and for the fully developed regime in condensation on the underside of slightly inclined surfaces.

An estimate of the accuracy with which the hydrodynamics were modeled may be inferred from the predicted values of the wavelengths. For both horizontal and inclined surfaces, the theoretical values are in error by about 25 per cent. This error is most likely due to the steady-state assumption.

(3) Experimentally observed heat-transfer rates for laminar film condensation on the underside of a horizontal surface are from 10 per cent to 15 per cent below those predicted by equation (22). This error remains about the same for values of the Rayleigh number ranging from $2{\cdot}0 \times 10^6$ to $2{\cdot}5 \times 10^8$.

Equation (22) is expected to maintain this accuracy for values of the Rayleigh number greater than 10^6 if the values of $k\Delta T/\mu h_{fg}$ and $c_p \Delta T/h_{fg}$ are much less than unity.

(4) Experimentally observed heat-transfer rates for film condensation on the underside of slightly inclined surfaces agree with equation (18) to within an error of 10 per cent. In addition to the above restrictions, this equation should be valid if $\tan\theta$ is small and if the flow is in the fully developed ridge state.

(5) All of the heat-transfer data from 20°

to 90° inclination fall about 10 per cent above the theoretical values predicted by equation (23). This suggests that, in the roll-wave regime, the net effect of interfacial waves remains roughly constant.

ACKNOWLEDGEMENT

This research was performed at the Heat Transfer Laboratory of the Massachusetts Institute of Technology and was supported by the National Science Foundation under Contract No. NSF GP-2402. The numerical work was performed at the Computation Center at the Massachusetts Institute of Technology. Support was provided for one of the authors (J. Gerstmann) as an N. S. F. Fellow.

REFERENCES

1. W. NUSSELT, The surface condensation of steam, *Z. Ver. Dt. Ing.* **60**, 541 and 569 (1916).
2. G. I. TAYLOR, The instability of liquid surfaces when accelerated in a direction perpendicular to their planes, I, *Proc. R. Soc.* **A 201**, 192–196 (1950).
3. V. D. POPOV, Heat transfer during vapor condensation on a horizontal surface, *Trudy Kiev. Teknol. Inst. Pishch. Prom.* **11**, 87–97 (1951).
4. J. GERSTMANN, Film condensation on the underside of a horizontal surface, S. M. Thesis, Dept. of Mechanical Engineering, M.I.T. (1964).
5. P. J. BERENSON, Transition boiling heat transfer from a horizontal surface, Technical Report No. 17, Division of Sponsored Research, M.I.T. (1960).
6. T. J. HANRATTY and A. HERSHMAN, Initiation of roll waves, *A. I. Ch. E. Jl* **7**, 488–499 (1961).
7. J. GERSTMANN and P. GRIFFITH, The effects of surface instabilities on laminar film condensation, Technical Report No. 5050-36, Dept. of Mechanical Engineering, M.I.T. (1965).
8. J. H. LIENHARD and P. T. Y. WONG, The dominant unstable wavelength and minimum heat flux during film boiling on a horizontal cylinder, *J. Heat Transfer* **86C**, 220–226 (1964).
9. L. M. TREFETHEN, personal communication, Tufts University, Medford, Mass. (September 1963).
10. F. BASHFORTH and J. ADAMS, *An Attempt to Test the Theories of Capillary Action by Comparing the Theoretical and Measured Forms of Drops of Fluid*, pp. 27–35. Cambridge University Press, Cambridge, England (1883).
11. W. M. ROHSENOW and H. Y. CHOI, *Heat, Mass and Momentum Transfer*, p. 240. Prentice-Hall, Englewood Cliffs, N.J. (1961).

Résumé—Les vitesses de transport de chaleur dans la condensation par film laminaire sur la face inférieure de surfaces horizontales et inclinées sont prévues en supposant que l'écoulement du condensat est le résultat quasi-permanent d'une instabilité limitée. Cette hypothèse rend possible la détermination de la forme finale de l'interface liquide-vapeur et ainsi prédit le coefficient moyen de transport de chaleur. Les mesures du coefficient de transport de chaleur obtenu en condensant le Fréon-113 s'accordent tout-à-fait avec les valeurs prévues par cette méthode.

On a observé plusieurs régimes distincts d'écoulement dans le film de condensat. Sur la face inférieure de surfaces horizontales, l'interface est décrite le mieux comme une instabilité de Taylor entièrement établie. Il existe trois régimes d'écoulement pour de faibles angles d'inclinaison. Près du bord d'attaque, l'interface est lisse et sans rides. A côté, se trouve une région d'ondes établies qui sont le mieux décrites sous la forme de gouttes allongées et de crêtes longitudinales. Comme les crêtes ont une amplitude croissante, des gouttes s'y forment et tombent ainsi de la surface. En-delà du point pour lequel les gouttes commencent à tomber, il existe un troisième régime qui peut être considéré comme un état entièrement établi, indépendant de la distance à partir du bord d'attaque de la surface. Pour des angles d'inclinaison modérés et jusqu'à une position verticale, de "rouleaux" apparaissent à une courte distance du bord d'attaque.

Zusammenfassung—Wärmeübergangsgeschwindigkeiten bei laminarer Filmkondensation an der Unterseite von horizontalen und geneigten Oberflächen werden bestimmt unter der Annahme, dass der Kondensatstrom das quasi-stationäre Ergebnis einer begrenzten Instabilität ist. Diese Annahme macht es möglich, die endgültige Form der Dampf/Flüssigkeits- Grenzschicht zu bestimmen und auf diese Weise den mittleren Wärmeübergangskoeffizienten zu ermitteln. Messungen des Wärmeübergangskoeffizienten bei Freon 113 stimmten sehr gut mit den so bestimmten Werten überein.

Verschiedene Erscheinungsformen des Kondensatfilms wurden beobachtet. An der Unterseite von horizontalen Flächen wird die Dampf/Flüssigkeits-Grenzfläche am besten als voll ausgebildete Taylor-Instabilität beschrieben.

Bei geringer Neigung zeigen sich drei Gebiete des Kondensatabflusses: In der Nähe der Oberkante ist die Oberfläche eben und glatt. Danach kommt ein Gebiet, in dem Wellen entstehen, am besten beschrieben als strömungsparallele Wulste von langgezogenen Tropfen. Während die Höhe der Wulste wächst, formen sich Tropfen an den Spitzen, die daraufhin abfallen. Unterhalb des Punktes, an dem die ersten

Tropfen fallen, existiert ein drittes Gebiet, welches wohl den voll entwickelten Zustand darstellt, unabhängig von der Entfernung von der Oberkante.

Bei grösseren Neigungen bis zur Vertikalen erscheinen kurz unterhalb der Oberkante "Roll-Wellen", die aussehen wie schuppenartig übereinandergeschobene Blätter.

Аннотация—При расчете теплообмена при ламинарной пленочной конденсации на нижней стороне горизонтальной и наклонной поверхностей принимается, что в результате связанной неустойчивости возникает квазистационарное течение конденсата. Это допущение позволяет определить конечную форму поверхности раздела жидкость-пар и, таким образом, рассчитать средний коэффициент теплообмена. Коэффициенты теплообмена, измеренные при конденсации фреона-113 хорошо согласуются с расчетными значениями, полученными предложенным методом.

В пленке конденсата наблюдалось несколько различных режимов течения. Граница раздела на нижней стороне горизонтальной поверхности лучше всего описывается с помощью теории неустойчивости Тейлора. При небольших наклонах поверхностей наблюдались три режима течения. Вблизи передней кромки поверхность раздела гладкая и волнообразования не наблюдается. Затем следует область, где возникают волны, которые лучше всего представить в виде удлиненных капель на продольных волнах. При увеличении амплитуды волн на гребнях образуются капли, которые затем срываются с поверхности. За точкой срыва первых капель находится третья область полностью развитого состояния, которая не зависит от расстояния от передней кромки поверхности. При средних углах наклона (вплоть до 90°) на небольшом расстоянии от передней кромки поверхности образуются «бегущие» волны.